

MODEL, SIMULATION AND EXPERIMENTS FOR A BUOYANCY ORGANIC RANKINE CYCLE

Jeroen Schoenmaker^{1*}, Pâmella Gonçalves Martins¹, Guilherme Corsi Miranda da Silva¹, Julio Carlos Teixeira¹

¹ Center for Engineering, Modelling and Applied Social Sciences – Federal University of ABC, Santo André, SP
CEP 09210-580 - Brazil

E-mail: jeroen.schoenmaker@ufabc.edu.br, jschoenmaker@gmail.com

* Corresponding Author

ABSTRACT

Organic Rankine Cycle (ORC) systems are increasingly gaining relevance in the renewable and sustainable energy scenario. Recently our research group published a manuscript identifying a new type of thermodynamic cycle entitled Buoyancy Organic Rankine Cycle (BORC) (Schoenmaker *et al.*, 2011). In this work we present two main contributions. First, we propose a refined thermodynamic model for BORC systems accounting for the specific heat of the working fluid. Considering the refined model, the efficiencies for Pentane and Dichloromethane at temperatures up to 100°C were estimated to be 17.2%. Second, we show a proof of concept BORC system using a 3 m tall, 0,062 m diameter polycarbonate tube as a column-fluid reservoir. We used water as a column fluid. The thermal stability and uniformity throughout the tube has been carefully simulated and verified experimentally. After the thermal parameters of the water column have been fully characterized, we developed a test body to allow an adequate assessment of the BORC-system's efficiency. We obtained 0,84% efficiency for 43,8°C working temperature. This corresponds to 35% of the Carnot efficiency calculated for the same temperature difference. Limitations of the model and the apparatus are put into perspective, pointing directions for further developments of BORC systems.

1. INTRODUCTION

Power plants based on Rankine cycle are responsible for about 85% of the electric energy production worldwide. It is arguably the most mature thermal energy technology.

In the scope of renewable and sustainable technologies, organic Rankine cycle (ORC) systems have drawn great attention (Imran *et al.*, 2018). These systems work with the same principle of operation of regular Rankine systems however substituting water for organic compounds and thus allowing the cycle to work efficiently in lower temperatures. As main advantages, ORC systems have simple structure, high reliability, low cost, easy maintenance and are increasingly being considered as a viable technology to convert low temperature heat into electricity (Rahbar *et al.*, 2017). One important research area in this field is the development of novel ORC architectures (Lecompte *et al.*, 2015).

On the other hand, buoyancy Rankine cycle is a modified Rankine cycle in which the turbine is replaced by an expander based on buoyancy force. It is worth noticing that the cycle itself is not necessarily organic, however the proposed technology is interesting as a renewable energy solution for low temperature applications.

Although there has been some research on the implementation of low temperature systems (Garcia *et al.*, 2018) and different expander architectures (Bao and Zhao, 2013, Qiu *et al.*, 2011, Lemort *et al.*, 2013) the authors of this manuscript have no knowledge of any experimental evaluation of a BORC architecture besides the experimental proof of principle being presented here.

In this context, BORC systems, as proposed by our group, are put forward as a contribution by being at the same time as a novel expander option for Rankine system and a new solution for distributed low-temperature energy generation.

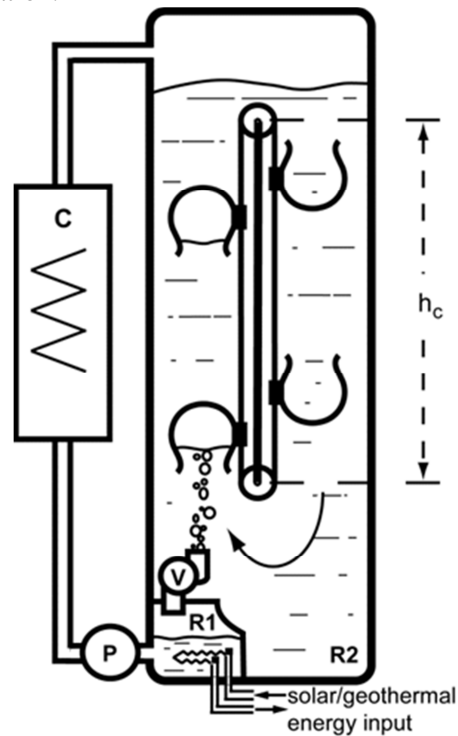


Figure 1: Sketch of a Buoyancy Organic Rankine Cycle (BORC) system. Elements indications are: P (pump), R1 (working fluid reservoir), R2 (column fluid reservoir) and C (condenser).

2. MODEL

Fig. 1 sketches a BORC system based on four main stages. First, the working fluid is pumped into a high pressure reservoir (R1). The pump is represented by element “P”. Second, the working fluid is heated and vaporized in R1. Third, the working fluid, in gaseous form, is expanded in the column fluid (usually water) reservoir R2 where mechanical energy of the buoyancy force is harnessed by a conveyor system. In the fourth and last stage, the working fluid is condensed back to its liquid state by the condenser “C”.

In this work we present a refined model to evaluate the efficiency of a BORC system. A previous model has been published elsewhere (Schoenmaker *et al.*, 2011). It departs from the general expression for the efficiency of a Rankine system:

$$\eta = \frac{W_C - W_P}{Q_{in}} \approx \frac{W_C}{Q_{in}} \quad (1)$$

where W_C is the work performed by the gas-filled inverted cups during the upward motion in reservoir R2, W_P is the work performed by the pump “P” and Q_{in} is the thermal energy input to the system. To evaluate W_C we considered the work done by the buoyancy force of the evaporated working fluid in the inverted cups. The buoyancy force originates from the difference in mass density (ρ) between the column fluid and the evaporated working fluid. Note that the buoyancy force increases as the cups move upwards due to the expansion of the working fluid as the column fluid pressure decreases. For a detailed calculation of W_C please refer to Schoenmaker *et al.*, 2011.

In our refined model, we consider a better estimation for Q_{in} , taking into account the heat capacity of the working fluid in the heating and vaporization process. Considering a classical thermodynamic point of view, a heat engine works by employing the temperature difference between a hot source and a cold reservoir. In a BORC system, the higher temperature is called “temperature of operation (T_{op})” and is defined by the temperature necessary to vaporize the working fluid at the bottom of the column

fluid reservoir. Consider that, the higher the column, the higher T_{op} will be as the pressure increases. After the working fluid performs work in the expander R2 it has to be liquefied in condenser C by cooling it down to the “liquefaction temperature T_l ”. Note that T_l is lower than T_{op} due to the difference in pressure where each of the processes of evaporation and liquefaction happens. Hence, once the working fluid is pumped into R1, Q_{in} has to account for the heat necessary to perform both: heat the liquid from T_l to T_{op} and evaporate it. In this case, the expression for Q_{in} is

$$Q_{in} = H_v(T_{op}) + c(T_{op} - T_l) \quad (2)$$

Where T_l is the temperature of the condensed working fluid while being pumped into reservoir R1. Thus, the final expression for the efficiency becomes

$$\eta = RT_{op} \left[\frac{\ln|\rho g h_c + P_0| - \ln|P_0|}{H_v(T_{op}) + c(T_{op} - T_l)} \right] \quad (3)$$

where c is the molar specific heat of the working fluid.

Fig. 2 depicts calculated efficiencies for two working fluid candidates: Pentane and Dichloromethane (DCM). Note that several assumptions are maintained in this model that has been originally adopted in the model described in (Schoenmaker *et al.*, 2011). Most importantly, the expansion of the working fluid in R2 happens in thermal equilibrium with the column fluid. As we are focusing on low temperature applications, we considered the lowest allowed temperature for the working fluid in gaseous state under column fluid pressure. Thus, the BORC system’s temperature of operation (T_{op}) is directly proportional to the water column height (h_c).

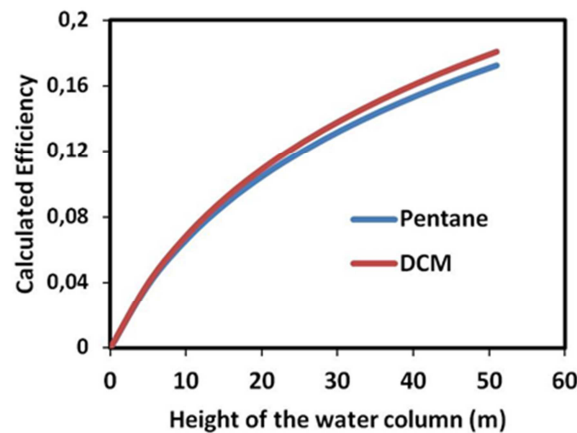


Figure 2: Calculated efficiencies for DCM and Pentane as a function of the height of the water column for an ideal BORC system according to eq. (3).

Some noteworthy aspects are apprehended from this refined model. Firstly, as expected, there is a small decrease of the overall efficiencies in comparison to previous model. Interestingly, DCM appears slightly more efficient than Pentane, inverting the trend obtained previously. Furthermore, the refined model presents results more consistent with other more established thermodynamic estimates (Imran *et al.*, 2018).

3. EXPERIMENTAL SETUP

We present a proof of concept BORC system using a 3 m tall, 0,062 m diameter polycarbonate tube as a column-fluid reservoir. Fig. 3 sketches the conceptual scheme of the column setup along with a picture of the actual assembly. We used water as a column fluid. Ideally, for a reliable experimental procedure, we should attain a stable and uniformly heated water column. A successful experiment also required a suitable test body. Initially we conceived a combined heating and temperature sensing

system to control the main parameters of the water column. As a test body, we outlined a mass attached to an expandable reservoir containing the working fluid.

The experimental test would ideally occur as follows: Initially the test body is inserted at room temperature (with the working fluid in liquid state) in the water column pre-heated to a controlled temperature of operation T_{op} . Once the test body is inserted, the mass drags the test body to the bottom of the water column. After some time, as the test body tends to establish thermal equilibrium with its surroundings, the working fluid evaporates, dragging the mass upwards to the top of the column, demonstrating a useful work obtained through buoyancy force.

Several tests and design adaptations were necessary in order to develop an adequate test body to assess the efficiency of the proof-of-concept BORG system. Fig. 4 depicts the final solution for the test body, showing each part separately. As an expandable container for the working fluid, we used a nitrile rubber balloon, as pentane demonstrated to be permeable in latex. To allow load adjustment, we used a variable number of 4,74g steel balls in our tests. To ensure proper control of the experiment, the working fluid was inserted in the uninflated balloon inside a pinholed centrifuge microtube (Eppendorf). Everything was suitably fitted inside a 15,7 cm tall and 4,0 cm diameter PVC tube capped in both ends. This tube worked as a limiting structure for the expansion of the balloon, thus avoiding the inflated test body to get jammed against the walls of the water column. As it is visible in the picture, we perforated the PVC tube and its caps to avoid air entrapment and allow water movement in and out of the tube enabling the overall change of the test body's density during the evaporation of the working fluid.

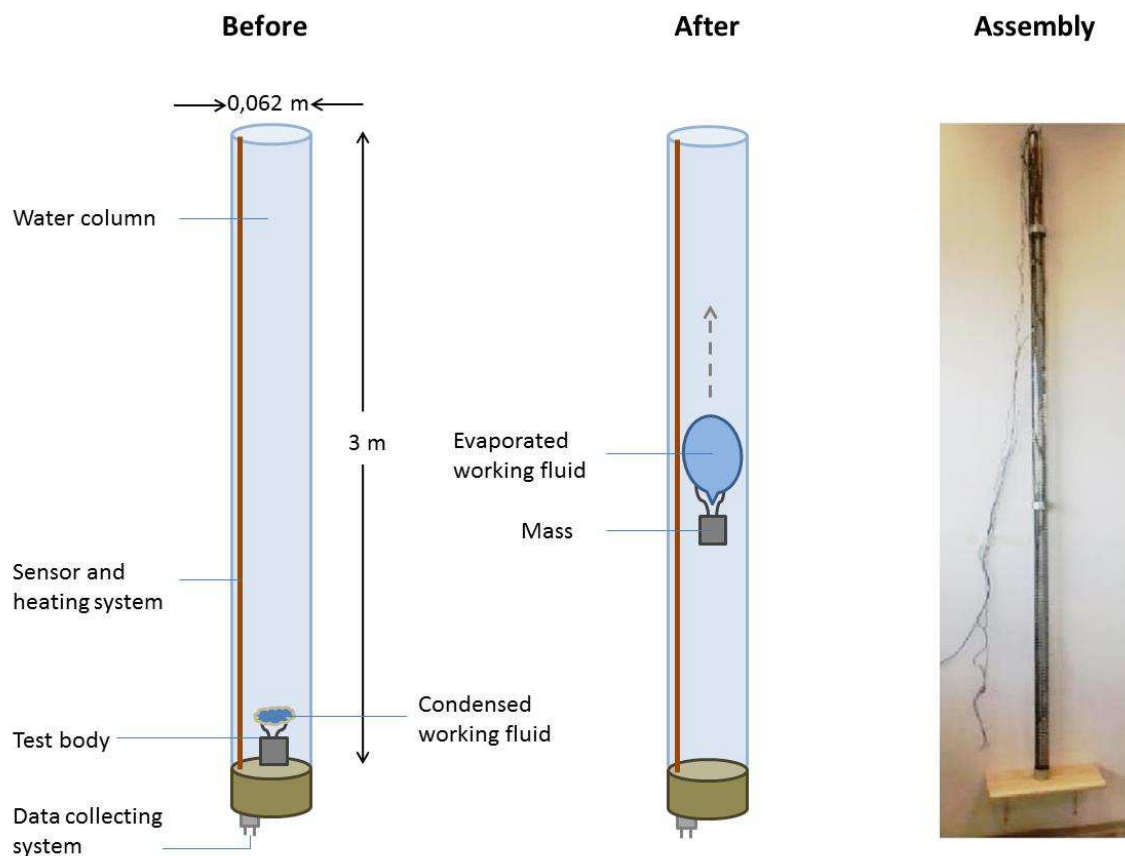


Figure 3: Sketch of the water column setup along with a picture of the actual column assembly. The sketch compares two different moments of a test: the test body as inserted in the system and after some time, when the test body reaches thermal equilibrium with its surroundings. In principle, the test body would consist of a mass attached to an expandable reservoir containing the working fluid in liquid state. Several design adaptations were necessary to the whole assembly.

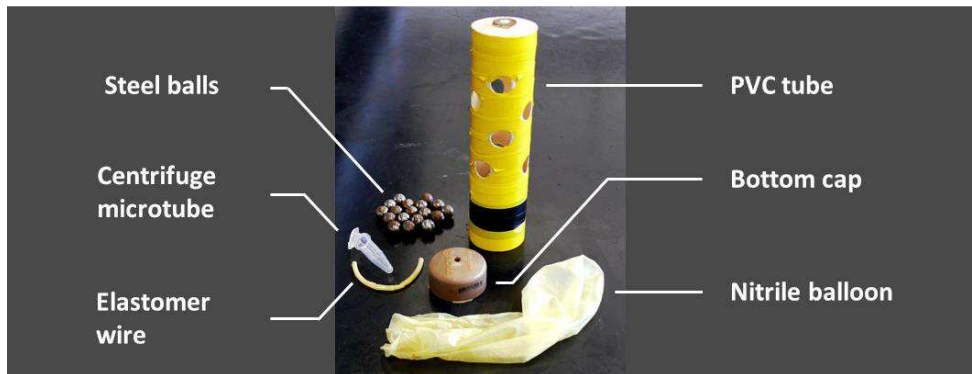


Figure 4: Picture of the test body showing each part separately. Parts consist of: PVC tube (covered with yellow and black tape) already with top cap, bottom cap (brown), nitrile balloon, steel balls, centrifuge microtube, elastomer wire (to seal the balloon).

To control the temperature of the water column, we used a joule heating ribbon throughout the entire height of the tube and three temperature sensors: bottom, middle and top positioned. The heating and sensing system was monitored by an Arduino platform interfaced to a computer (Arduino, 2018).

4. RESULTS AND DISCUSSION

The thermal stability and uniformity throughout the tube has been carefully simulated and verified experimentally.

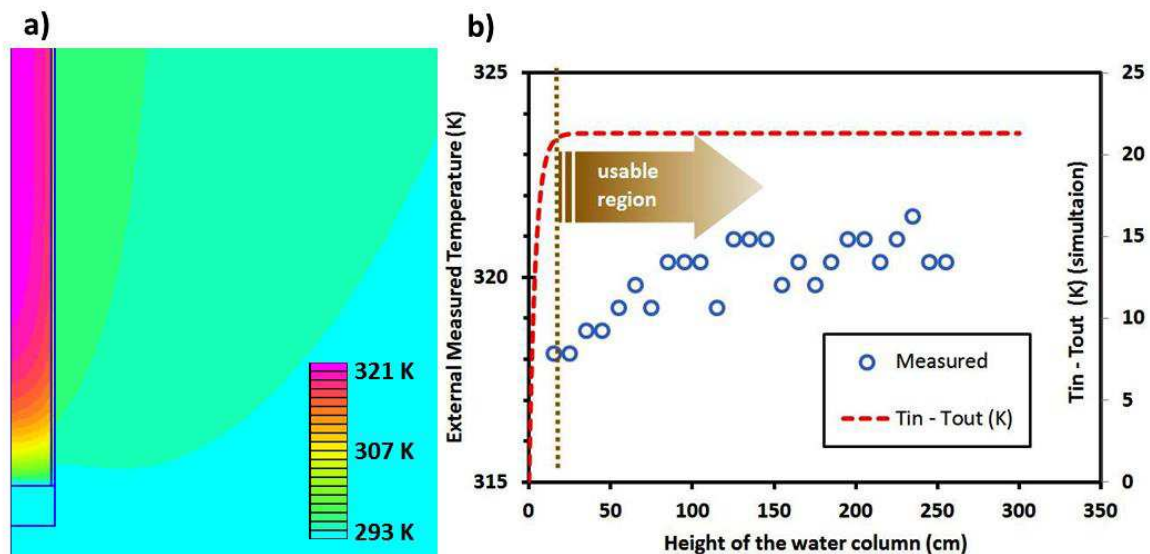


Figure 5: a) Heat loss simulation for the water column kept 30°C above room temperature. Image depicts the bottom 55 cm of the tube. b) Measurement of the temperature uniformity along the height of the tube (blue open circles) in comparison with the simulated temperature difference profile inside the tube and immediately outside the tube (dashed red line). The model predicts a proportional temperature gradient in and out of the tube.

Relevant parameters of the water column, such as temperature distribution and heat loss have been simulated using Finite Element Method Magnetics (FEMM) software (Meeker, 2015). The simulation was performed using the axial symmetry and considering conduction and convection heat transfer factors. For a 30°C temperature difference between the water column and its surroundings, simulations estimated a total heat loss of 88 W with a time constant of 92 min. We experimentally verified these values using the joule heating system, obtaining a temperature stable water column with 97,4 W power supply. Moreover, simulations showed significant temperature gradient at the bottom ~20 cm of the column (see Fig. 5a). This temperature difference has been detected by the sensors

placed outside the tube. The temperature profile has been characterized by measuring the temperature of the tube externally in 25 different positions along the height of the tube and considering that there is proportionality between inside and outside polycarbonate wall temperatures, after the heat loss process reached steady state. This proportionality assumption is consistent with simulations (Fig. 5b). The bottom temperature gradient has shown to be an unsurmountable problem, even with the rearrangement of the joule heating ribbon and several attempts to thermally insulate the bottom aluminum cap of the column tube. Furthermore, due to water convection, the heating system demonstrated to be a source of significant instabilities.

After the thermal behavior of the water column has been consistently characterized, we verified that removing the heating system altogether, maintaining just the top and bottom temperature sensors, was the better procedure. Water was poured already in high temperature inside the tube and experimental tests were taken during the long period of temperature decline. As each procedure was undertaken within 1 minute, we assumed constant temperature during each test given the thermal inertia of the system (time constant). Moreover, we reduced the usable height of the water column to just 2,5 m in order to avoid inconsistencies due the bottom thermal gradient.

According to our BORG model, the working and column fluids are in thermal equilibrium during the expansion process (third phase of the BORG process). Our experiments focused on test trials tending to the lowest possible temperature of operation, estimated to be 41,5°C for a 2,5 m water column.

For the resulting system, given the size of the test body and quantized loading scheme, we calculated the optimum mass and working fluid ratio to be 139,55 g (18 steel balls plus mass of the test body structure) and 0,6 ml of n-pentane (measured with micropipette) respectively. Prior to each procedure we determined the volume of the test body using liquid displacement technique in a graduated cylinder. Several successful tests have been performed. The one with the lowest temperature has been performed with $T_{op} = 43,8^\circ\text{C}$ with initial volume of the test body of 85 ml. The test demonstrated an efficiency of 0,84% (Fig. 6), that is about half of the modeled efficiency for the tested height and 35% of the Carnot Efficiency calculated for the experimental conditions.

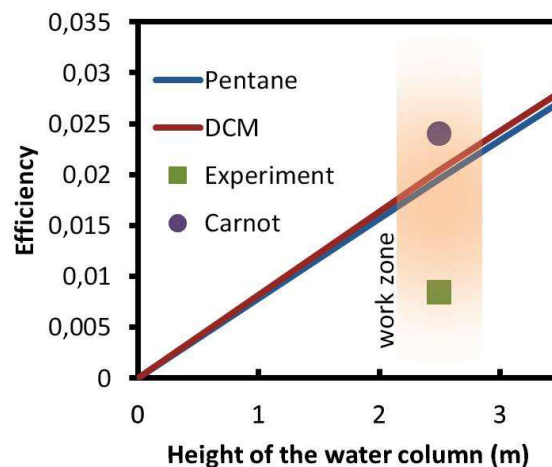


Figure 6: Best experimental result for the efficiency of our proof of principle BORG system (green square) plotted together with the calculated efficiency for Pentane and DCM working fluids (same data as Fig. 2 blown up to the scale of our system) along with Carnot efficiency calculated for $T_{op} = 43,8^\circ\text{C}$ (purple circle).

The main limitation of our system is related to its design. Buoyancy force is based on density gradient and has been estimated based on the amount of weight the test body can drag upwards. Our test body has a fixed mass for each procedure. The change in water density along the height of the tube is negligible. On the other hand, the density of the test body is dependent on the expansion of the pentane vapor, which is strongly dependent of the pressure of the water column, reaching its minimum on the top of the tube. Another limitation is the overall size of the system, which is considerably small. Note that tests were undertaken using working fluid quantities of about 0,5 ml. This aspect renders the system considerably subject to sources of uncertainties which are avoidable otherwise. We are currently working on a larger system considering a proper design to avoid the above mentioned limitations.

5. CONCLUSIONS

The model for estimating the efficiency of a BORC system put forward in previous publication has been refined in this work. Considering the new model, the efficiencies for Pentane and Dichloromethane at temperatures up to 100°C were estimated to be 17,2%. A successful proof of principle set up has been modeled and constructed. We obtained 0,84% efficiency for $T_{op} = 43,8^{\circ}\text{C}$, corresponding to 35% of a Carnot cycle working in the same temperature difference. Keeping the same proportionality, this represents a BORC system working with 6,1% efficiency in temperatures under 100°C. Limitations of the model and the apparatus are put into perspective, pointing directions for further developments of BORC systems.

NOMENCLATURE

BORC	buoyancy organic Rankine cycle	
c	molar specific heat of the working fluid	$\text{J.mol}^{-1}.\text{K}^{-1}$
C	condenser	
DCM	Dichloromethane	
g	standard acceleration due to gravity	m.s^{-2}
h_c	height of the conveyor belt	m
$H_v(T_{op})$	enthalpy of vaporization at BORC's operating temperature (T_{op})	J.mol^{-1}
P	pump	
P_0	atmospheric pressure	Pa
Q_{in}	thermal energy input to the system	J
R1	working fluid reservoir	
R2	column fluid reservoir	
T_{op}	temperature of operation of R2	K
T_{in}	temperature inside the polycarbonate test tube	K
T_{out}	temperature outside the polycarbonate test tube	K
T_l	temperature of the condensed working fluid when pumped into R1	K
W_C	work performed by the gas-filled inverted cups in R2	J
W_P	work performed by the pump "P"	J
η	efficiency	
ρ	density of the column fluid	kg.m^{-3}

REFERENCES

- Arduino. 2018: <<http://www.arduino.cc/>> accessed in 13 Apr 2018.
- Bao, J., Zhao, L., 2013, A review of working fluid and expander selections for organic Rankine cycle, *Renewable and Sustainable Energy Reviews*, vol. 24 p. 325–342 <http://dx.doi.org/10.1016/j.rser.2013.03.040>
- Garcia, S. I., Garcia, R. F., Carril, J. C., Garcia, D. I., 2018, A review of thermodynamic cycles used in low temperature recovery systems over the last two years, *Renewable and Sustainable Energy Reviews* vol. 81p. 760–767 <http://dx.doi.org/10.1016/j.rser.2017.08.049>
- Imran, M., Haglind, F., Asim, M., Alvi, J. Z., 2018, Recent research trends in organic Rankine cycle technology: A bibliometric approach, *Renewable and Sustainable Energy Reviews* vol. 81 p. 552–562 <http://dx.doi.org/10.1016/j.rser.2017.08.028>
- Lecompte, S., Huisseune, H., van den Broek M., Vanslambrouck, B., De Paepe, M., 2015, Review of organic Rankine cycle (ORC) architectures for waste heat recovery, *Renewable and Sustainable Energy Reviews* vol. 47 p. 448–461

- Lemort, V., Guillaume, L., Legros, A., Declaye, S., Quoilin, S., 2013 A comparison of piston, screw and scroll expanders for small scale Rankine cycle systems, *Proceedings of the 3rd international conference on microgeneration and related technologies*;
- Meeker, D., 2015, Finite Element Method Magnetics Version 4.2 User's Manual, October 25, 2015, available in <<http://www.femm.info/Archives/doc/manual42.pdf>> Accessed in 13/04/2018
- Qiu, G., Liu, H., Riffat, S., 2011, Expanders for micro-CHP systems with organic Rankine cycle, *Applied Thermal Engineering* vol.31 p. 3301-3307 doi:10.1016/j.applthermaleng.2011.06.008
- Rahbar, K., Mahmoud, S., Al-Dadah, R. K., Moazami, N., Mirhadizadeh, N. S. A., 2017, Review of organic Rankine cycle for small-scale applications, *Energy Conversion and Management* vol. 134 p. 135–155
- Rahbar, K., Mahmoud, S., Al-Dadah, R. K., Moazami, N., Mirhadizadeh, S. A., 2017, Review of organic Rankine cycle for small-scale applications, *Energy Conversion and Management* vol. 134 p. 135–155
- Schoenmaker, J., Rey, J. F. Q., Pirola, K. R., 2011, “Buoyancy Organic Rankine cycle”, *Renewable Energy* vol. 36 p. 999-1002 doi:10.1016/j.renene.2010.09.014

ACKNOWLEDGEMENT

This work was supported by UFABC (undergrad fellowships for Pâmella Martins and Guilherme Silva)